The research in this project is carried out in the frame of a FLAG ERA project, GRIFONE (Graphitic films of group III nitrides and group II oxides: platform for fundamental studies and applications.) Coordinator is Anelia Kakanakova, Linköping Sweden, partner: Filippo Gianazzo, CNR Catania, Italy.

The aim of this international project is the growth of 2D nitride layers between graphene and SiC as well as the growth of layers onto graphene/SiC templates.
Both aims are very challenging and the whole project has a high risk.

What we could fulfil first that was the growth of nitrides over the graphene. That however, was achieved on patterned surface of graphene/SiC. We could publish a keynote paper in physica status solidi in the first period of this project.

The graphene/SiC templates were grown also in the frame of the project by high-temperature sublimation technique (also known as thermal decomposition of SiC), which results in epitaxial graphene layers on Si-face of SiC.
Then our partner made some basic experiment with the hydrogenation of graphene, what passivates the SiC surface and makes that quasi free standing and makes possible the intercalation of indium, gallium, or aluminium. That process needed some optimization as well.

Then first at about the half of the project In_2O_3 intercalated layer could be detected instead of the InN we wanted to grow. Then only islands of GaN could be grown on graphene/SiC.

We achieved a breakthrough in both major subjects in 2018. First of all we could figure out that despite many unsuccessful depositions of Al_2O_3 a solid and homogeneous layer can be grown, when he graphene is only a monolayer thick. Another key influencing parameter is the epitaxial monolayer of graphene on SiC and the buffer layer below. Our manuscript discussed the role of the buffer layer as well, was submitted to Advanced Materials Interfaces, accepted and published.

Then using our new aberration corrected TEM (installed in June 2018) we could prove that we have 2D InN in a new set of the samples grown by MOCVD. This was again a breakthrough. Based on this result we requested the prolongation of the project to the end of 2019, what was approved by NKFIH (The foreign partners did the same at their home funding offices. Once we could really clearly show the InN (for example in Z contrast images in STEM) we started to compose a manuscript. However, when we wanted to determine the bandgap of the 2D InN by EELS (Electron Energy Loss Spectrometry) we failed, as it is very difficult to make such a measurement at a few eV values. Then we tried to make STM measurements (STS Scanning Tunneling Spectroscopy), practically by taking I-V curves in our institute. When we overcame some technical limitations we could make a reliable measurement what gave us a direct bandgap of 2 eV (+-0.1). This is a great difference from the value of 0.7 eV characteristic for the bulk, or thick layers. Moreover, it is in agreement with our expectations. With this result InN became a member of the wide bandgap semiconductors, where up to now it was placed because it was easy to grow a ternary alloy with that.

Our publication strategy was delayed in 2019, because we had to understand how we can grow InN and indium oxide and we had to prove that really we have nitrogen in our two atomic layer thick grown structures. We wanted to avoid the need of any withdraw of our papers, what is not so rare in the world today.

The indium containing 2D layers were grown at 700°C from the same precursors. Therefore in all processes InN was formed we believe, but the layers was oxidized and the nitrogen content lost when the cooling down was carried out without further feeding of the nitrogen source (ammonia). This means that we can immediately turn our 2D-InN to In2O3, what is a very well known semiconducting material as well with a bandgap of 2.9 eV. However, our conductive

AFM measurements showed that the bandgap of the grown 2D oxide is about 4 eV, actually easy to accept because of quantum confinement. The paper on indium oxide is written and ready for submission to Advanced Materials, most probably we will submit that next week. The manuscript is attached to this report.
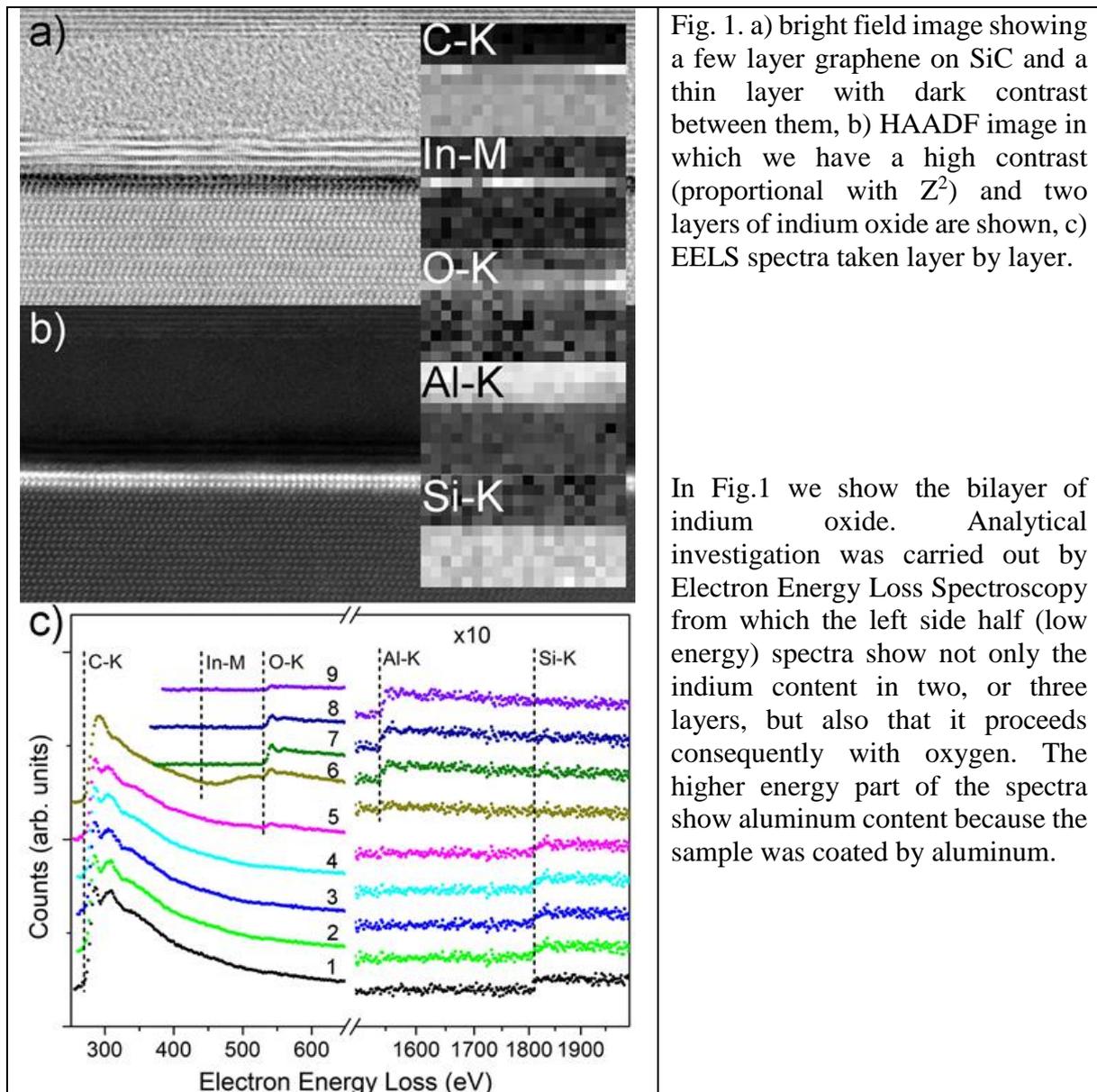
Fig. 1. a) bright field image showing a few layer graphene on SiC and a thin layer with dark contrast between them, b) HAADF image in which we have a high contrast (proportional with Z^2) and two layers of indium oxide are shown, c) EELS spectra taken layer by layer.

In Fig.1 we show the bilayer of indium oxide. Analytical investigation was carried out by Electron Energy Loss Spectroscopy from which the left side half (low energy) spectra show not only the indium content in two, or three layers, but also that it proceeds consequently with oxygen. The higher energy part of the spectra show aluminum content because the sample was coated by aluminum.

InN layer

When the nitrogen was fed not only during the growth, but also during the cooling down process InN layers have been received. One of those layers are shown with the top morphology in the next figure together with some electrical data received from the conductive AFM measurements. What is very important that about 90% of the surface is intercalated and InN is formed.
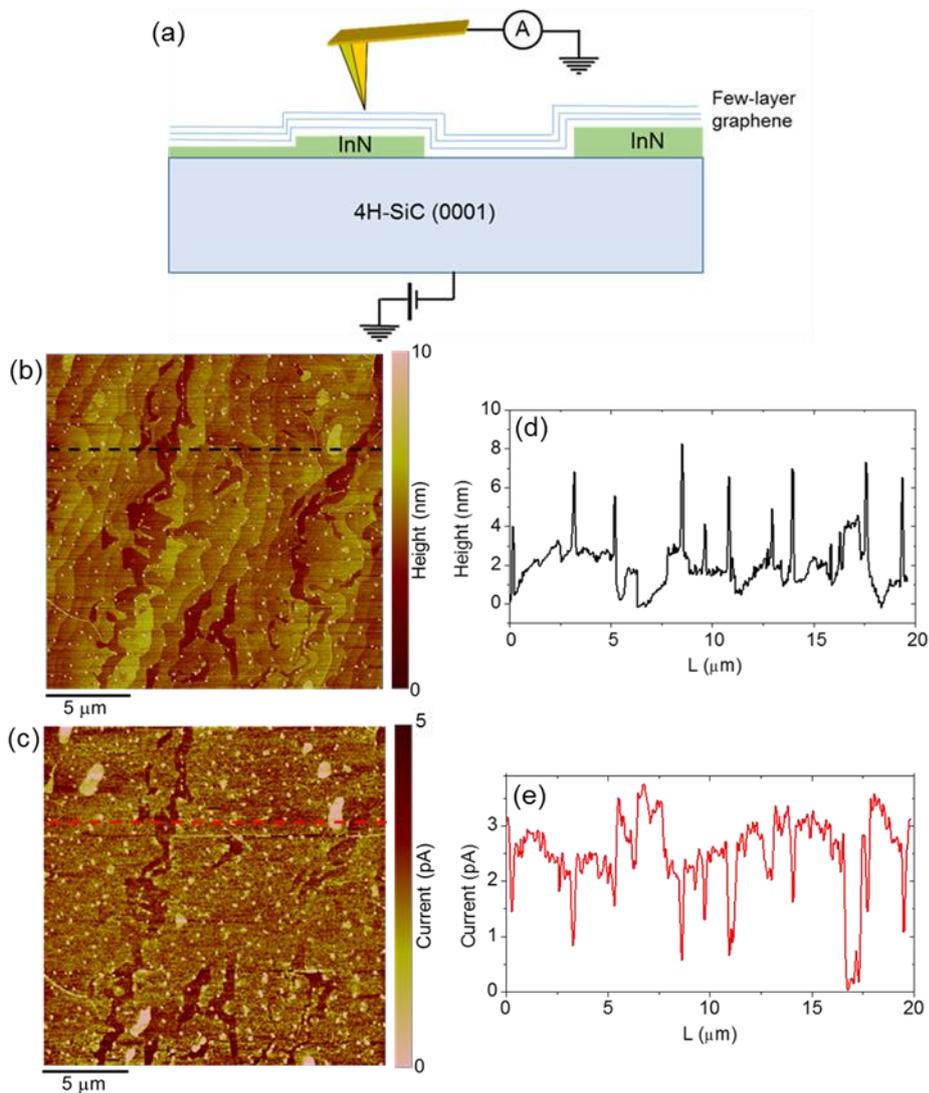
Fig. 2: Conductive AFM morphology and current line scans of the next InN sample, it is clear that, although there is some inhomogeneity, at least 90% of surface is intercalated and InN is formed.

Fig.3 shows a representative high resolution image of InN intercalated. The image was taken at 200 keV.
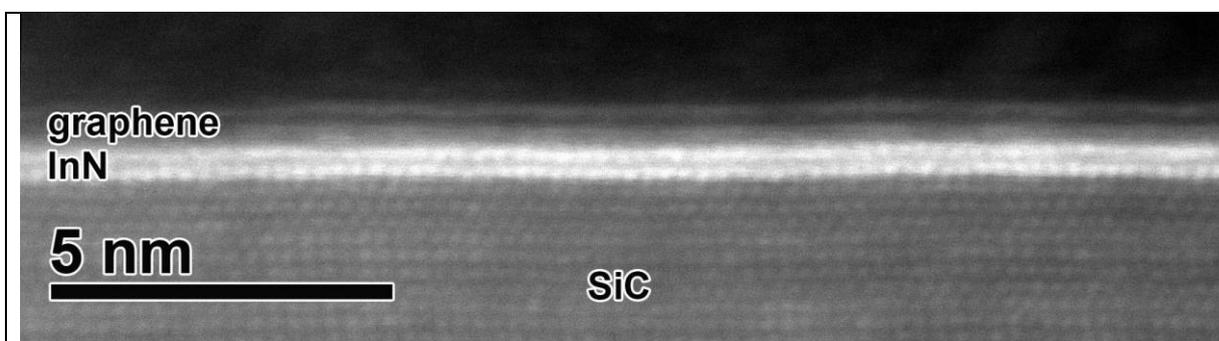
Fig. 3. STEM HAADF image taken on the graphene/SiC template intercalated with indium and ammonia. The bilayer of InN with high intensity Z contrast and the covering bilayer of graphene is clearly seen.
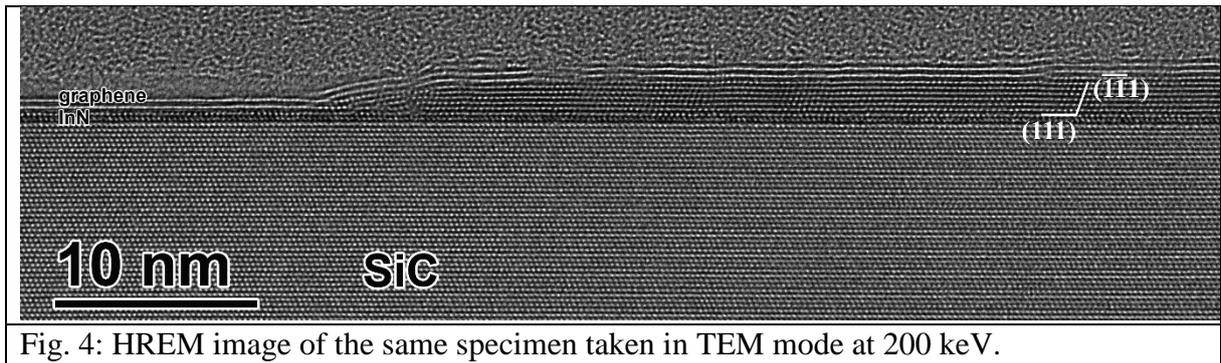
Fig. 4: HREM image of the same specimen taken in TEM mode at 200 keV.

The first study of the grown samples at 200 keV did confirm the indium and nitrogen content of the thin layer, especially the indium appears with bright contrast in the HAAADF image of Fig. 3. Moreover the EDS analysis we discuss later confirmed the presence of nitrogen in the thin layer.

Several TEM lamellas were prepared from the same sample and investigated even taking overview images. Ased on that study we conclude that the major regions of the grown InN are composed of two layers, there are regions less than 10% of the surface where intercalation did not occur therefore InN is not grown and finally there are occasionally a few nm thick regions of InN as well, like it is shown on the right part of Fig. 4. Growing InN via RF MBE (Molecular beam epitaxy) D. Ishimaru, AG. Bhuiyan and A. Hashimoto, J. Appl. Phys. 126, 045301 (2019) also found that the growth turns to 3D mode after the 3rd layer is grown despite the layer by layer growth of MBE.

It is obvious that the material in our case that thick region is not hexagonal, but can be indexed as cubic InN, two of the (111) type planes are marked in the image.
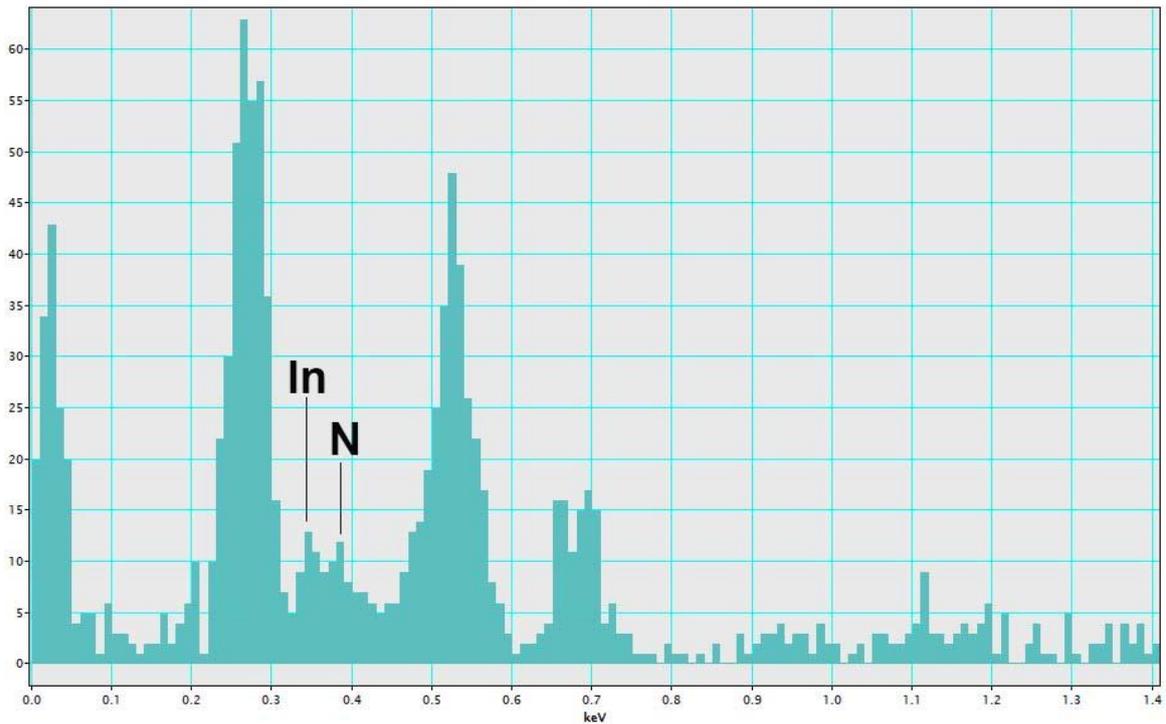
Fig.5: EDS spectrum with clear indium and nitrogen content taken on 2D InN.

Detection of nitrogen by EDS is not easy and someone has to be careful when indium is also present. The nitrogen peak, without tilting the specimen to the EDS detector was separated from the close indium M_{alpha} peak and the spectrum is shown in Fig. 5.

Also having access to a probe corrected microscope (via successful ESTEEM3 application) we could take some ABF (Annular Bright Field) images as well with a collection angle from 11 to 22 mrad. Characteristically for this technique, all the atoms are dark in the image and the low mass atoms can visualize as well. The top image in Figure 6 is an atomic resolution overview from which the bottom image is magnified. In the bottom image in Figure 6, the indium atoms are the large very dark discs, while the nitrogen atoms are also seen with grey contrast, some of them being marked by blue circles in the image. (Having access to that microscope also made possible to make a lot of analysis at 60 keV lowered electron energy, when we are sure graphene is left intact. However, for the better resolution those measurements were repated at 200 kV.)
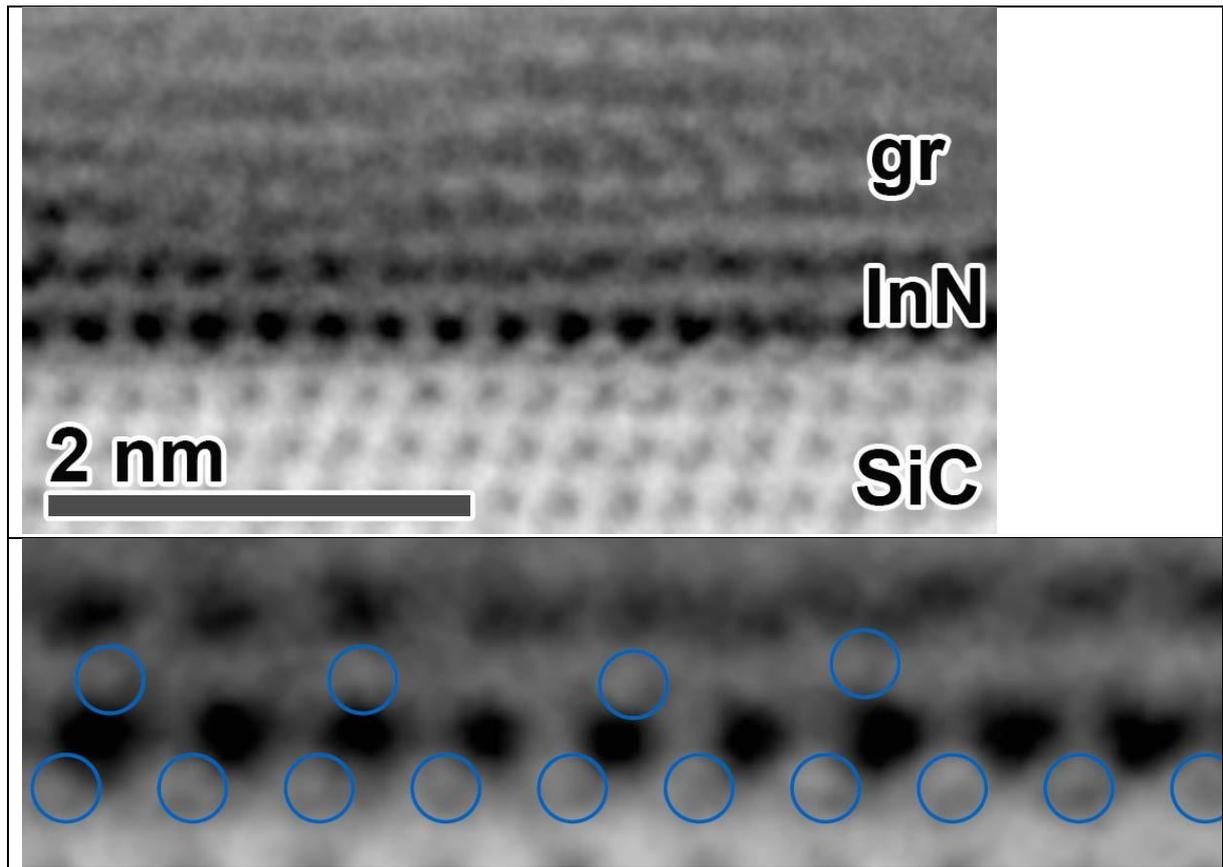
Fig. 6 ABF images of InN

Measurements in order to determine the bandgap of our InN regions were carried out by Scanning tunneling microscopy (STM) taking I-V curves from the top of the sample (*Scanning tunneling spectroscopy, STS*). Each STS measurement was repeated 10 times and the average was calculated. In Fig 7 is shown a characteristic STS curve from which the forbidden bandgap of 2 ± 0.1 eV was extracted for our 2D InN. This value differs a lot from the 0.7 eV of the bulk (or thick) InN crystals, however it is logical to observe a larger bandgap due to the quantum confinement. We believe that our experimental data are in agreement with the simulations published by V. Wang et al. (V. Wang, Z. Q. Wu, Y. Kawazoe, and W. T. Geng, J. Phys. Chem. C 2018, 122, 6930−6942).
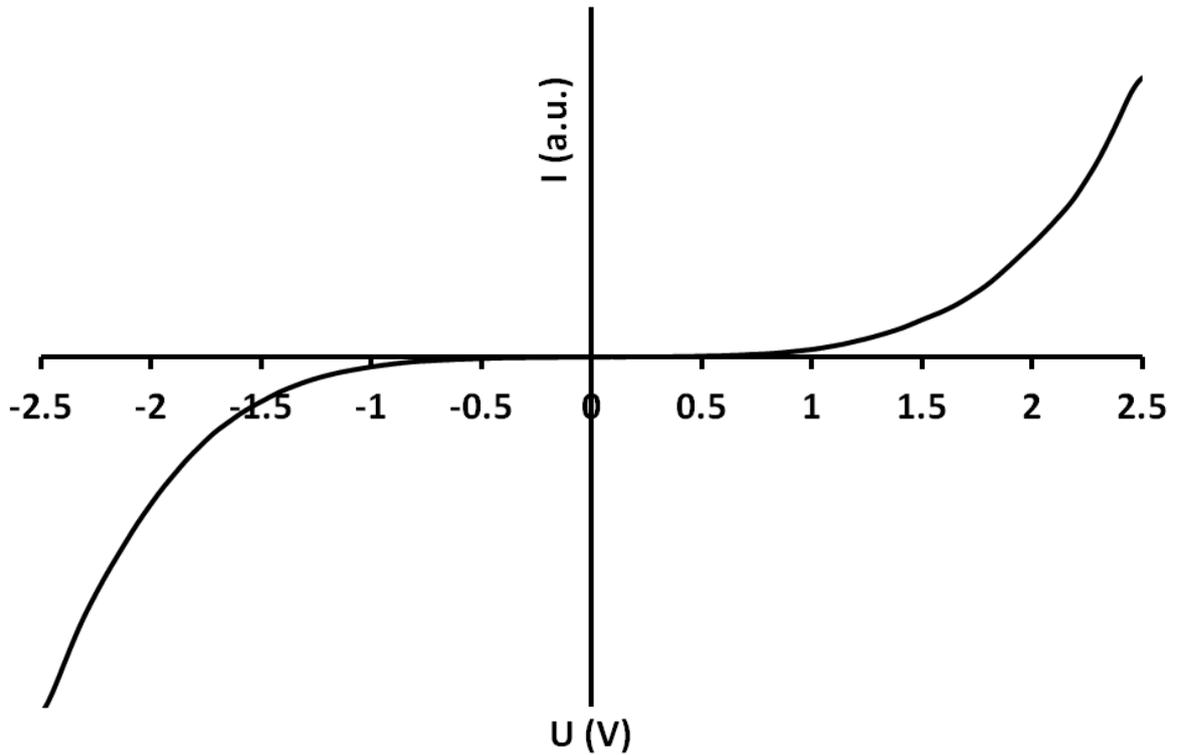
Fig. 7. Characteristic STS curve taken on 2D InN

The second manuscript with the results on 2D InN is under preparation and will be submitted soon to a journal with high impact.

While the indium intercalated structures are worldwide new and no one reported on 2D InN, or indium oxide there are more data already on 2D GaN till this paper was published: *Z. Y. Al Balushi, K. Wang, R. K. Ghosh, R. A. Vilá, S. M. Eichfeld, J. D. Caldwell, X. Qin, Y.-C. Lin, P. A. DeSario, G. Stone, S. Subramanian, D. F. Paul, R. M. Wallace, S. Datta, J. M. Redwing, and J. A. Robinson, Nature Materials, 2016, 15, 1166.*
Probably second time we also could make 2D GaN intercalated between graphene and SiC and we also plan a third paper submission on that in the future.

Material Proposal for 2D Indium Oxide by Tuning the Formation of 2D Indium Nitride

Anelia Kakanakova-Georgieva*, Filippo Giannazzo, Giuseppe Nicotra, Rositsa Yakimova, Per Å.O. Persson, and Béla Pécz

Dr. A. Kakanakova-Georgieva, Prof. R. Yakimova, Prof. P. Å. O. Persson
Department of Physics, Chemistry and Biology (IFM), Linköping University,
581 83 Linköping, Sweden
E-mail: anelia.kakanakova@liu.se
Dr. F. Giannazzo, Dr. G. Nicotra
Consiglio Nazionale delle Ricerche, Istituto per la Microelettronica e Microsistemi,
Strada VIII, n. 5, Zona Industriale, I-95121, Catania, Italy
Dr. B. Pécz
Centre for Energy Research, Institute of Technical Physics and Materials Science,
Konkoly-Thege M. út 29-33., Budapest, 1121, Hungary

(**Abstract**) *Maximum length 200 words, Written in the present tense and impersonal style*

Exceptional and diversified performance and exercising transformative influence on the modern technology and society can be elicited through the realization of well-established semiconductor materials at the 2D limit. We report first-time evidence for the formation of two-dimensional indium oxide (2D InO_x) with two-dimensional indium nitride (2D InN_x) as a precursor whereby control and bonding transformation is harvested through intercalation and kinetics at the interface between hydrogen passivated SiC substrate and quasi-free-standing graphene in metal organic chemical vapor deposition (MOCVD) processes. The initial development has been triggered by exploring the innovative material concept for "graphitic" films of group III nitrides and advanced by indicating an opportunity for a multifunctional material platform involving 2D group III nitrides and 2D group III sesquioxides.

(**Main Text Paragraphs**) *The maximum length of a Communication is four journal pages — approximately 3000 words (including main text, experimental section, references, and captions) and three display items (figures, tables, or schemes). Longer papers will be accepted only in exceptional cases if their quality warrants special consideration.*

The expansion of fundamental scientific knowledge, supported by development of theoretical approaches, deposition strategies, and advanced characterization, drives rational design of materials at the nanoscale. This is recognized as a materials science platform that brings about conceptually new performance with well-established semiconductor materials, which build up the fundamental components of virtually any electronic device in use by our modern society, have been subjected to a variety of nanostructures.

Nanostructures such as two-dimensional quantum wells, one-dimensional quantum wires/rods, and zero-dimensional quantum dots can be stated as being among the most typical examples whereby at least one dimension of the nanostructure is limited by the exciton Bohr radius, e.g., ~ 8 nm for InN, as compared to 2.4 nm for GaN, and 1.4 nm for AlN in the material system of group III nitrides.[1] Indium oxide from the material system of group III sesquioxides [2] provides an extra compelling example. In addition to the realization of quantum confinement effects, one-dimensional nanostructures represented by nanowires with diameters below 4 nm greatly promote the performance of chemical/biosensors and transparent electronics.[3] Array of obliquely aligned InN nanowires has been demonstrated for the fabrication of notably efficient nanogenerators to convert mechanical energy into electricity.[4]

Yet exceptional and diversified performance of the modern-technology-relevant InN can be elicited through its realization at the 2D limit by exploring the innovative material concept for "graphitic" films of group III nitrides.[5-8] "Graphitic" films of group III nitrides with the

2

planar trigonal sp^2 coordination of their constituent atoms act as precursors to the polar (0001)/(000-1) thin films of group III nitrides with the common tetrahedral sp^3 coordination of their bonds.[5] The sp^2-bonded planar structure has been calculated as the most thermodynamically stable when applied to few-layer films of several wurtzite semiconductor materials including AlN and GaN.[5] Relaxation of the sp^2-bonded planar structure for thicker films of these materials, and involvement of a certain charge transfer, yields the characteristic sp^3-bonded three-dimensional wurtzite structure.[5] The stability of the sp^2-bonded planar structure with respect to the characteristic sp^3-bonded three-dimensional structure is number-of-layer dependent. In the case of AlN, respectively, GaN and InN, this maximum set of layers was calculated to be as many as about twenty, respectively, ten and eight, and to be further extended by applying tensile strain.[9] 2D AlN and GaN have been studied extensively from the perspective of first principles calculations, so that structural optimization of their free-standing monolayer and few-layer conformations, stability analysis, electronic structure, and optical properties have been presented in a focused review.[10] On the other hand, there is a fragmentary theoretical knowledge about 2D InN. The first experimental evidence of "graphitic" films of AlN built up from 12 sp^2-bonded monolayers was obtained under scanning tunneling microscopy conditions on catalytic substrates of Ag(111),[11] which thus corroborated the theoretical calculations. The first experimental manifestation for the formation of 2D GaN was obtained under metal organic chemical vapor deposition (MOCVD) conditions via "migration-enhanced encapsulated growth technique" utilizing epitaxial graphene.[12]

We report, for the first time, formation of a two-dimensional indium nitride (2D InN$_x$) by MOCVD processes which were submitted to an ultimate control over the deposition kinetics contributed by the recognized implementation of the interface between hydrogen passivated SiC substrate and quasi-free-standing graphene. Within the framework of deposition kinetics

controlled MOCVD processes, and by tuning the formation of 2D InN_x, we advance a

material proposal for two-dimensional indium oxide (2D InO_x) which establishes the

realization of a new class of 2D materials. Mutually compatible 2D semiconductor materials

can be developed by MOCVD, with a range of structural and electronic properties, and a

distinctive potential for tunability as to drive exceptional transformations in the design and

performance of novel 2D electronics devices.

Intercalated layers of indium (In) at the interface between hydrogen passivated SiC substrate

and quasi-free-standing graphene giving origin to 2D InO_x were recorded by parallel

acquisition of annular bright-field (ABF-) and high-angle annular dark field (HAADF-)

scanning transmission electron microscopy (STEM) images in combination with electron

energy loss spectroscopy (EELS) spectrum imaging. In **Figure 1**a, b, the ABF- and HAADF-

STEM images are shown at atomic resolution, respectively. The SiC is located at the bottom

(zig-zag appearance) with two atomic layers of In, seen as dark dots in Figure 1a and bright

dots in Figure 1b, immediately nucleated on the SiC. Above the intercalated layers of In, four

layers of graphene are visible, particularly in Figure 1a and partly in Figure 1b. (Then follows

an amorphous structure and finally a single crystal layer at the top of the images, both of them

just from the aluminium deposited in order to prevent the original surface during the focused

ion beam preparation of the TEM lamella.) To investigate the elemental composition across

the interface, EELS spectrum imaging was applied. The results are shown in Figure 1c. The

spectrum imaging was recorded across the interface and laterally integrated to reduce noise.

Each spectrum in Figure 1c can be viewed as a line scan across the interface with

approximately 1 nm spacing between the spots. At the bottom of the spectrum imaging, only

C and Si are visible from their K-edges with onset at ~280 and ~1840 eV energy loss, as

indicated in the graph. At the interface, seen already in spectrum (5), both In and O appears as

seen from their M and K edges, at ~440 and ~530 eV energy loss respectively. The In-M can

be observed in (5) as a change of the background slope but it is most apparent in (6) together with O. Note also the apparent change in character of the C-K fine structure in (6) as the C bond is changed from the SiC sp^3 type to sp^2 type in graphene. This spectrum is integrated across both the In and graphene layers, and indicates that In appears to bond with O. In (7) and above, C is only present as residual contamination, and the spectra has been background subtracted after the C-edge for practical purposes. The background subtracted elemental signals were integrated across a window between the edge onset and +40 eV, in order to produce the C, In, O, and Si elemental maps of the spectrum imaging, and the results are overlaid in Figure 1a, b.

While there is an apparent intercalation of In atoms into the graphene/SiC interface, the MOCVD process involves the delivery of strongly bonded metal organic precursor species such as $(CH_3)_3In$ into contact with the graphene surface. The precursor trimethylindium $(CH_3)_3In$ bears common characteristics with the other typical metal organic precursors implemented for the MOCVD of group III nitrides including trimethylaluminum $(CH_3)_3Al$. The strength of the bond between the metal atom and the methyl group is the strongest in the $(CH_3)_3Al$ and for this precursor we have performed, for the first time, ab initio molecular dynamics (AIMD) of atomic-scale surface reactions with graphene surface providing understanding of atomistic and electronic processes responsible for the supply of Al adatoms via precursor/graphene surface reactions.[13] These AIMD simulations can be used as a model to rationalize the atomistic pathways and dissociative patterns for the supply of In adatoms on the graphene surface and their intercalation consequent to $(CH_3)_3In$/graphene collisions. High lifetime and surface diffusivity have been obtained for the adsorbed Al atoms in the respective AIMD simulations, with the underlying reactions predominantly evolving via CH_3-In=CH_2 dissociation on graphene after the initial elimination of a methane molecule.[13] It is important to note that in an alternative branch of reactions, C adatoms derive from the CH_2 group after

its dehydration at the graphene surface.[13] The supply of C adatoms to the graphene surface is being associated with weakening of the C-C bonds as to the vicinity of existing defects, referenced mainly to pentagons and Stone-Wales defects, thus creating larger holes in the bonding network facilitating intercalation. Alternatively, the increased reactivity of unsaturated bonds in the carbon sheet may be expected to contribute the dissociative NH_3 adsorption on the graphene surface.

The above reasoning, reflecting paths for supply of individual metal atoms from strongly bonded metal organic precursors, subsequent functionalization of graphene and intercalation, motivates the scheme of precursor delivery in our deposition runs. The metalorganic precursor of $(CH_3)_3In$ is first supplied to the graphene surface followed by NH_3. The scheme of precursor delivery involved in total 3 cycles each consisting of alternating $(CH_3)_3In$ with NH_3 followed by an extra time of joint delivery of $(CH_3)_3In$ and NH_3 before the flow of the precursors was cut simultaneously with the switching off the RF heating power for the execution of the cooling down stage of the overall MOCVD process. An inherent effect of this cooling down stage was the formation of 2D InO_x, Figure 1, which may be considered in relation to the formation of precursor 2D InN_x.

To submit this presumption to a test, subsequent experiments were performed and the cooling down stage of the overall MOCVD processes was executed in the continuous flow of NH_3 and H_2. This deposition process indeed resulted in the formation of 2D InN_x. This is illustrated via a typical bilayer structure of InN in **Figure 2**. InN was imaged very easily with high brightness on HAADF images, but in this case ABF technique was applied with a collection angle from 11 to 22 mrad. Characteristically for this technique, all the atoms are dark in the image and the low mass atoms can visualize as well. The top image in Figure 2 is an atomic resolution overview from which the bottom image is magnified. In the bottom image in Figure

2, the indium atoms are the large very dark discs, while the nitrogen atoms are also seen with grey contrast, some of them being marked by blue circles in the image. The nitrogen content of these layers was also confirmed by EDS analysis.

In confirmation of our presumption, the continuous flow of NH_3 and H_2 and their interrelated dissociative adsorption on the graphene surface prevents any deficiency of N atoms, including during the cooling down stage, and the outcompeting of N atoms by oxygen atoms in the creation of bonds with the In atoms. Oxygen species are inevitably present as MOCVD environmental contaminations and In is particularly selective to the formation of indium oxide.[14]

Nanoscale resolution current mapping by conductive atomic force microscopy (CAFM) [15] was employed to evaluate the lateral uniformity of intercalated 2D InO_x, as well as to get insight in the electronic properties of the graphene/2D InO_x/SiC heterostructure. The experimental setup for CAFM measurements is schematically illustrated in **Figure 3**a. A Pt-coated tip is scanned on the surface while a bias is applied to the sample backside, and the current flowing vertically across the heterostructure is collected by a current sensor with pA sensitivity connected to the tip. Figure 3b and c shows a representative morphology image and the corresponding current map acquired on a large area (20 µm × 20 µm) by applying a DC bias of -1 V to the sample. The stepped morphology in Figure 3b originates from the step-bunching of SiC during high temperature growth of epitaxial graphene. The current map in Figure 3c clearly shows distinct areas with lower and higher injected current, which were associated to the 2D InO_x-intercalated and not-intercalated epitaxial graphene regions, respectively. The histogram of current values extracted from this map is reported in Figure 3d, from which the percentages of InO_x-intercalated (~ 55.75%) and not intercalated (44.25%) graphene were estimated. A higher resolution morphology and current map collected at the

boundary between these different regions are reported in Figure 3e and f, along with representative height and current line-scans. The measured step height (~ 1.3 nm) between the InO_x - intercalated and not-intercalated areas is in close agreement with the thickness of InO_x obtained from cross-sectional STEM images. A reduction of the injected current by more than a factor of 6 is observed due to the presence of this ultra-thin barrier layer. By assuming direct tunneling of electrons from the SiC conduction band across this layer, the conduction band minimum of 2D InO_x was estimated to lie ~ 0.15 eV above that of 4H-SiC. Noteworthy, according to the electron affinity values of crystalline bulk In_2O_3 (~ 4.2 eV) and 4H-SiC (~ 3.1 eV), for a thick In_2O_3 film the conduction band is expected to lie ~ 1.1 eV below that of SiC. The very different conduction band misalignment for the 2D InOx indicates the occurrence of significant quantum confinement effects, also observed for other 2D materials with respect to their bulk counterparts.[12]

In summary, we report first-time evidence and material characteristics for the formation of 2D InO_x with 2D InN_x as a precursor whereby control and bonding transformation is harvested through intercalation and kinetics at the interface between hydrogen passivated SiC substrates and suspended graphene. It makes an appealing case for the MOCVD realization of "palette" of 2D materials from the material system of group III sesquioxides and group III nitrides and thus creating opportunity for an alternative multifunctional 2D semiconductor materials platform.

Experimental Section

Epitaxial graphene: The developed MOCVD processes implement the interface between hydrogen passivated SiC substrate and suspended graphene. The epitaxial graphene on SiC was fabricated by high-temperature sublimation technique in house by the growth protocol developed by R. Yakimova.[16, 17] SiC has hexagonal crystal structure and is stacked along the

c-axis layer by layer to form a certain polytype, in this case it is 4H-polytype with the (0001) basal plane exposed. This presumes that the substrate is cut perpendicularly to the c-direction which leads to substrates with polar faces: Si face (0001) and C face (000-1) terminated. We are using Si face (0001) grown graphene. A specific feature of our epitaxial graphene is that as grown on the Si face (0001), it contains a buffer layer (zero-layer graphene) which is an interfacial layer between the SiC substrate and the 1st graphene layer, i.e. it is preceding the formation of graphene. Typical size of the samples was 7x7mm^2.

Metal organic chemical vapor deposition (MOCVD): The MOCVD processes were developed in a horizontal-type hot-wall MOCVD reactor (GR508GFR AIXTRON) by implementing 4H-SiC (0001) substrates with epitaxial graphene. The rational deposition of 2D semiconductor materials built up from group III nitrides motivates the choice of MOCVD by being the prime deposition route to the formation of epitaxial materials for application in electronic devices and on various substrates including SiC.[1, 18] It is of essence that SiC (0001) surfaces with epitaxial graphene can be hydrogen intercalated under MOCVD conditions for passivation of the Si dangling bonds.[19] Regular termination of the surface dangling bonds is required to accomplish deposition of 2D materials on 3D substrates as demonstrated on the example of molecular beam epitaxy of naturally layered transition metal dichalcogenides on sulfur-terminated GaAs(111) and GaSe on hydrogen-terminated Si(111);[20] and as being of recognized contribution for the formation of 2D GaN on epitaxial graphene under MOCVD.[12] We have developed hydrogen intercalation of epitaxial graphene in a range of MOCVD processes which is evidenced by the appearance on a typical Raman spectra of a characteristic phonon peak ascribed to the formation of Si–H bonds.[21] Epitaxial graphene was heated up in the gas-flow of H_2 gas to the temperature of 700ºC. The gas-flow rate of the H_2 carrier gas was at 25 slm. The reactor was operated at a pressure of 200 mbar. Trimethylindium, $(CH_3)_3In$, and ammonia, NH_3, were employed as precursors at the gas-flow

rate of 0.000875 slm and 2 slm, respectively. The scheme of precursor delivery involved in total 3 cycles each of about 3 minutes and consisting of alternating $(CH_3)_3In$ with NH_3 followed by an extra time of 10 minutes of joint delivery of $(CH_3)_3In$ and NH_3. A purge flow of H_2 separated the alternating flows of $(CH_3)_3In$ with NH_3 in each cycle. The formation of the atomically thin layers of indium nitride involved that the flow of NH_3 and H_2 continued during the cooling down stage of the overall MOCVD process, while they were cut during the formation of the atomically thin layers of indium oxide.

Atomic Force Microscopy (AFM): The morphology of the samples was evaluated by tapping mode AFM using Si probes and a DI3100 equipment with a Nanoscope V controller. Conductive atomic force microscopy (C-AFM) was further employed to probe vertical current injection through the epitaxial graphene/2D InO_x/SiC interface. Current mapping and local current-voltage (I-V) analyses were carried out using Pt-coated Si tips with 5 nm curvature radius.

Scanning transmission electron microscopy (STEM): Transparent TEM lamella was cut by FIB (Focussed Ion Beam) in which the energy of Ga ions was reduced to 2 keV. In order to keep the top region of the sample intact first carbon, then platinum layer was deposited inside a dual beam FEI SCIOS2. Amorphous carbon coating is advantageous when the TEM/STEM microscope alignment is done. TEM was carried out in a FEI THEMIS 200 microscope equipped with an image corrector at 200 keV. STEM investigation of the epitaxial graphene/2D InN_x/SiC hetrostructure was carried out in a JEOL ARM probe corrected microscope also equipped with an EELS (Electron Energy Loss Spectrometer) and EDS (Energy Dispersive Spectrometer. STEM investigation of the epitaxial graphene/2D InO_x/SiC hetrostructure was carried out in an FEI Titan microscope at 300 kV

Acknowledgements

References

[1]   I. M. Watson, *Coordination Chemistry Reviews* **2013**, *257*, 2120.

[2]   H. von Wenckstern, *Adv. Electron. Mater.* **2017**, *3*, 1600350.

[3]   G. Shen, B. Liang, X. Wang, H. Huang, D. Chen, and Z. L. Wang, *ACS Nano* **2011**, *5*, 6148.

[4]   N.-J. Ku, C.-H. Wang, J.-H. Huang, H.-C. Fang, P.-C. Huang, and C.-P. Liu, *Adv. Mater.* **2013**, *25*, 861.

[5]   C. L. Freeman, F. Claeyssens, and N. L. Allan, *Phys. Rev. Lett.* **2006**, *96*, 066102.

[6]   E.F. de Almeida Junior, F. de Brito Mota, C.M.C. de Castilho, A. Kakanakova-Georgieva, and G. K. Gueorguiev, *Eur. Phys. J. B* **2012**, *85*, 48.

[7]   C. Bacaksiz, H. Sahin, H. D. Ozaydin, S. Horzum, R. T. Senger, and F. M. Peeters, *Phys. Rev. B* **2015**, *91*, 085430.

[8]   R. B. dos Santos, F. de Brito Mota, R. Rivelino, A. Kakanakova-Georgieva, and G. K. Gueorguiev, *Nanotechnology* **2016**, *27*, 145601.

[9]   D. Wu, M. G. Lagally, and F. Liu, *Phys. Rev. Lett.* **2011**, *107*, 236101.

[10]   D. Kecik, A. Onen, M. Konuk, E. Gürbüz, F. Ersan, S. Cahangirov, E. Aktürk, E. Durgun, and S. Ciraci, *Appl. Phys. Rev.* **2018**, 5, 011105.

[11]   P. Tsipas, S. Kassavetis, D. Tsoutsou, E. Xenogiannopoulou, E. Golias, S. A. Giamini, C. Grazianetti, D. Chiappe, A. Molle, M. Fanciulli, and A. Dimoulas, *Appl. Phys. Lett.* **2013**, *103*, 251605.

[12]   Z. Y. Al Balushi, K. Wang, R. K. Ghosh, R. A. Vilá, S. M. Eichfeld, J. D. Caldwell, X. Qin, Y.-C. Lin, P. A. DeSario, G. Stone, S. Subramanian, D. F. Paul, R. M. Wallace, S. Datta, J. M. Redwing, and J. A. Robinson, *Nature Materials*, **2016**, *15*, 1166.

[13]   D.G. Sangiovanni, G.K. Gueorguiev, and A. Kakanakova-Gueorguieva, *Phys. Chem. Chem. Phys.* **2018**, *20*, 17751.

[14]   H. F. Liu, N. L. Yakovlev, D.Z.Chi, and W.Liu, *J. Solid State Chemistry* **2014**, *214*, 91.

[15]   F. Giannazzo, G. Greco, F. Roccaforte, C. Mahata, and M. Lanza, in *Electrical Atomic Force Microscopy for Nanoelectronics* (Ed: U. Celano), Springer Nature, Cham, Switzerland **2019**, Ch. 10.

[16]   R. Yakimova, *Mater. Sci. Forum* **2010***, 645-648,* 565.

[17]   R. Yakimova, *Nature Nanotechnology* **2010**, *5,* 186.

[18]   M. Feneberg, N. T. Son, and A. Kakanakova-Georgieva, *Appl. Phys. Lett.* **2015**, *106*, 242101.

[19]   C. Riedl, C. Coletti, T. Iwasaki, A. A. Zakharov, and U. Starke, *Phys. Rev. Lett.* **2009**, *103*, 246804.

[20]   A. Koma, *J. Cryst. Growth* **1999**, *201/201*, 236.

[21]   I. Shtepliuk, I. G. Ivanov, T. Iakimov, R. Yakimova, A. Kakanakova-Georgieva, P. Fiorenza, and F. Giannazzo, *Materials Science in Semiconductor Processing* **2019**, *96*, 145.

Figure 1. a) High resolution bright field and b) HAADF images of the indium oxide bilayer on SiC covered by graphene, c) EELS spectra taken layer by layer
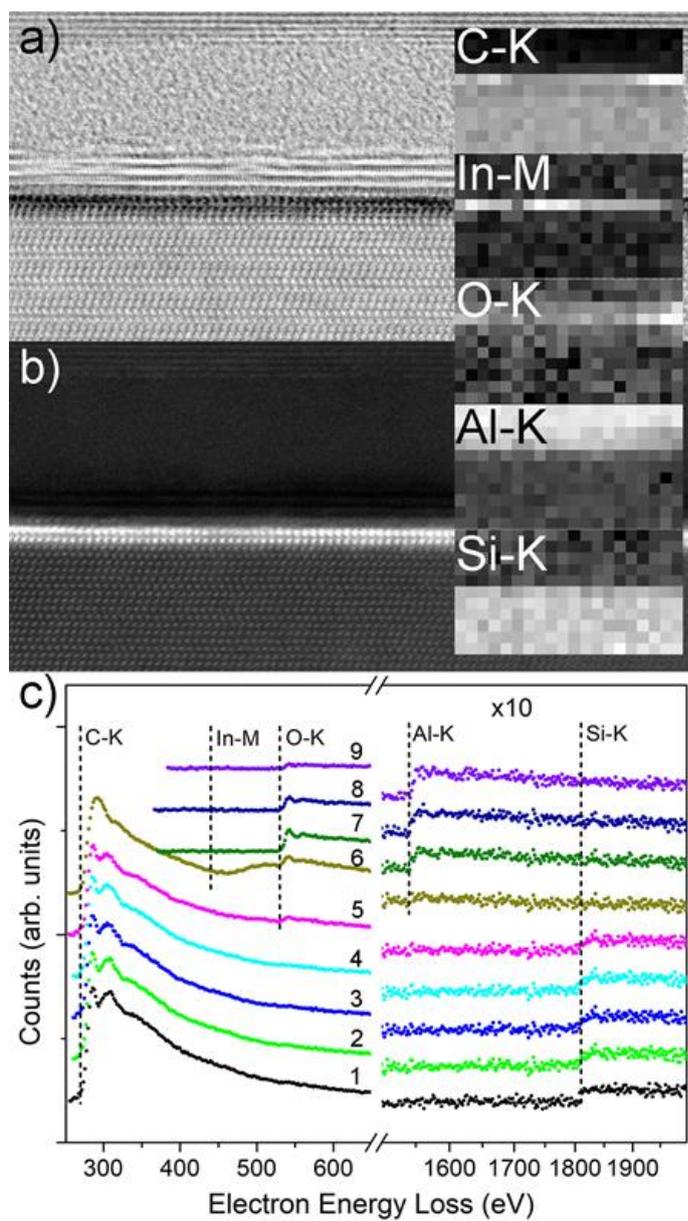
Figure 2. Annular bright field (ABF) images collected with aberration-corrected STEM near the (11-20) zone axis resolving nitrogen atoms in the graphene/2D InN_x/4H-SiC(0001) heterostructure.
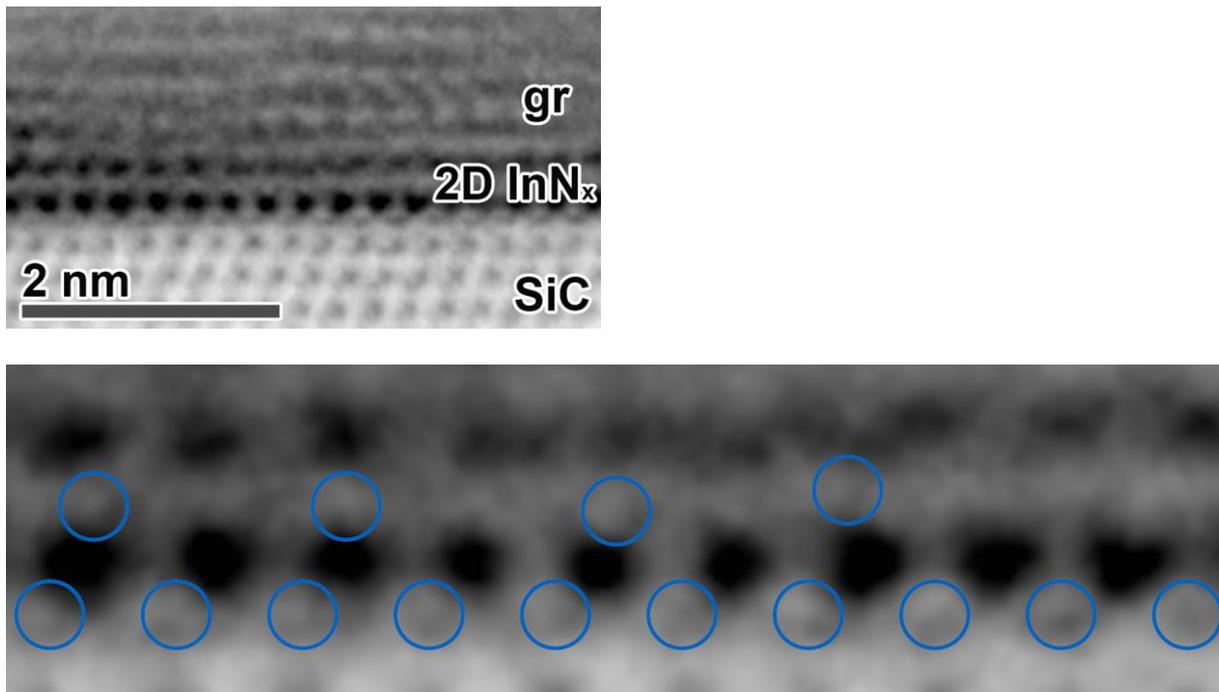
Figure 3. (a) Schematic illustration of the CAFM setup (b) Morphology and (c) current map acquired on large area (20 μm ×20 μm) to probe the uniformity of InO_x intercalation. (d) Histogram of the current distribution extracted from the CAFM map and percentage of InO_x

intercalated graphene. (e) High resolution morphology (f) current map along with representative height and current linescans showing the InO$_x$ thickness and the current drop associated to this ultrathin barrier.
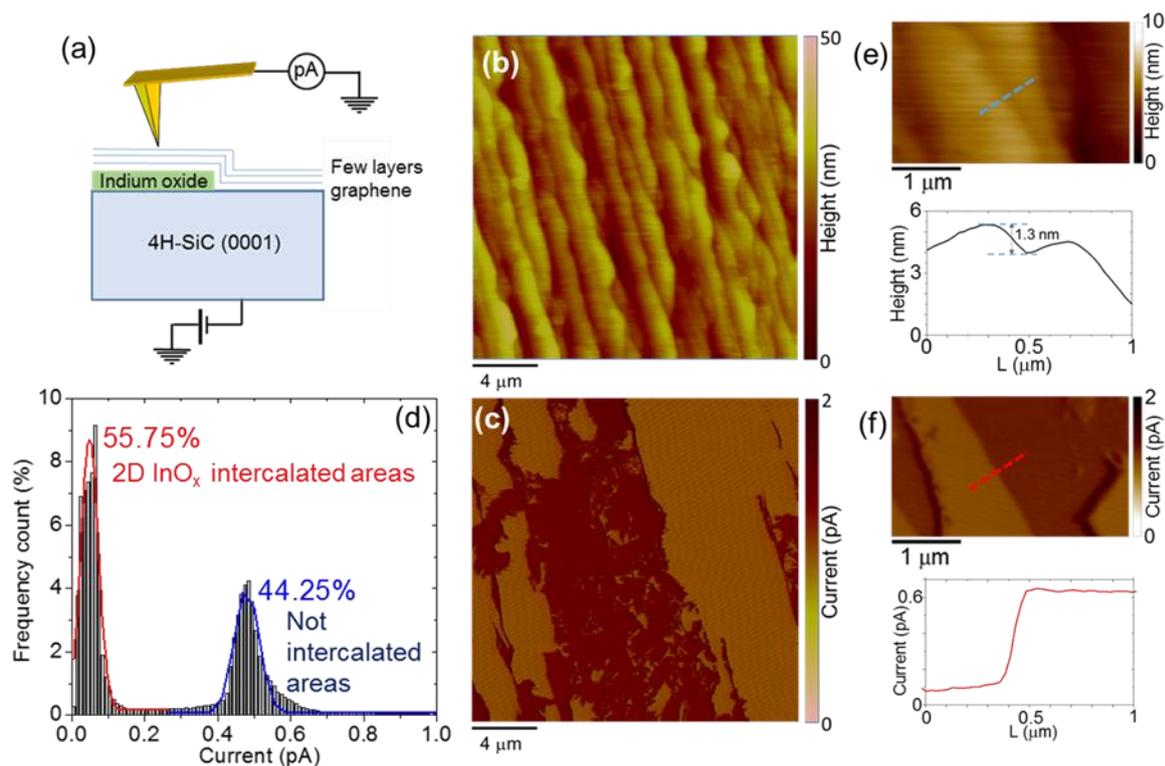
The table of contents entry should be 50−60 words long, *and the first phrase should be bold. The entry should be written in the present tense and impersonal style.*

Keyword

C. Author 2, D. E. F. Author 3, A. B. Corresponding Author* ((same order as byline))

Title *((no stars))*

*ToC figure ((Please choose one size: 55 mm broad × 50 mm high **or** 110 mm broad × 20 mm high. Please do not use any other dimensions))*